Available online at www.sciencedirect.com
ScienceDirect
Journal of Sound and Vibration 321 (2009) 270–285
JOURNAL OF SOUND AND VIBRATION
www.elsevier.com/locate/jsvi

Free and forced flexural vibration analysis of cantilever plates with attached point mass

S.D. Yu*

Department of Mechanical and Industrial Engineering, Ryerson University, 350 Victoria Street, Toronto, Ontario, Canada M5B 2K3

Received 21 February 2008; received in revised form 19 September 2008; accepted 22 September 2008
Handling Editor: S. Bolton
Available online 6 November 2008

Abstract

In this paper, the method of superposition or the Gorman method is employed to obtain an analytical solution for free and forced vibrations of cantilever plates carrying point masses. The free lateral vibration analysis is carried out by employing five building blocks—four for the cantilever plate and one for the point mass. Computed eigenvalues show that the proposed scheme is accurate and convergent for free vibration analysis. Once the eigen-analysis is completed, the modal summation method is then used to deal with the base-induced lateral vibration of cantilever plates carrying a point mass. Effects of mass ratios and locations of the point mass on eigenvalues and modal participation factors are investigated for square and rectangular plates.

1. Introduction

Many energy scavenging devices are designed to capture the ambient energy surrounding the electronics and convert it into usable electrical energy. There are a number of sources of harvestable ambient energy including vibration [1]. According to Anton and Sodano [2], the structural and biological communities have placed an emphasis on scavenging vibrational energy with piezoelectric materials although many other sources of energy can also be effectively used. When a piezoelectric material is strained, it produces an electric field. Cantilever piezoelectric panels and beams carrying heavy concentrated masses are commonly used in some portable and wireless devices as an efficient and compact way to generate electricity from base motion induced by human movement. The piezoelectric panels consist of a passive elastic material (core) and two thin layers of piezoelectric materials. For this type of application, the thickness of the cantilever structure is very small compared to its length and width. The in-plane material properties of the piezoelectric material and the core are essentially isotropic. Therefore, the classical plate theory can be used to deal with lateral vibration and design of thin piezoelectric panels.

Heavy masses are usually placed near the free edge of a cantilever plate to reduce the fundamental frequency of the plate-mass system to a desired value. To eliminate the electrical cancellation due to higher modal

*Tel.: +1 416 979 5000x7687; fax: +1 416 979 5265.
E-mail address: syu@ryerson.ca

0022-460X/$ - see front matter © 2008 Elsevier Ltd. All rights reserved.
doi:10.1016/j.jsv.2008.09.042

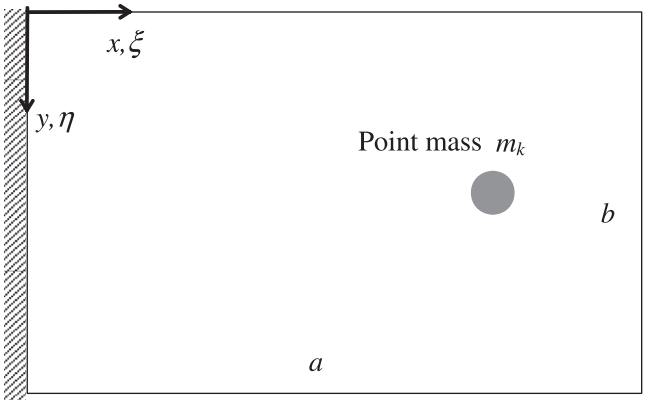

Fig. 1. A cantilever plate carrying a point mass.

responses, the dynamic strains on either side of the piezoelectric panel must be homogeneously tensile or compressive. Participation of high vibration modes adversely affects the net charge production, and is not desirable. To ensure that maximum amount of electrical energy is produced for a given base motion, the fundamental frequency of the panel is designed to be near the source frequency; frequencies of higher vibration modes are designed to be away from the fundamental frequency. Design of frequencies for promoting fundamental mode response requires free and forced vibration analyses of cantilever plates carrying point masses (Fig. 1).

There are several papers dealing with free vibration problems of cantilever plates carrying single and multiple concentrated masses. Ciancio et al. [3] studied the free vibration problem of a cantilever anisotropic rectangular plate carrying a concentrated mass using the Rayleigh–Ritz method, or the Ritz method recommended by Leissa [4] for use in the vibrations research community after a thorough review of historical notes by Lord Rayleigh and Walter Ritz concerning the development of the energy-based approximate method. Singhal and Gorman [5] studied free vibration of point-supported plates with attached masses. Chiba and Sugimoto [6] presented a comprehensive study of coupled and decoupled free vibration analyses of an isotropic cantilever thin rectangular plate carrying a spring–mass system attached on an arbitrary point by using the Ritz method. As a limiting case, they also investigated the influence of an attached mass by setting the spring constant to be infinity.

To obtain an analytical solution for free vibration of a plate subjected to various boundary and interior conditions, one needs to construct a series of building blocks, for which exact analytical solutions may be obtained easily using the generalized Levy method. For a rectangular plate, a Levy type solution can be obtained if it has a pair of opposite edges subjected to combinations of simple support and slip-shear boundary conditions. For a rectangular plate having homogeneous classical boundary conditions on its edges, four building blocks are required. The number of building blocks is equal to the number of edges whose boundary conditions are neither simple support nor slip-shear.

By taking advantage of symmetry and antisymmetry of modes with respect to the centerline running normal to the clamped edge, Gorman [7] studied one half of a cantilever plate. This approach reduces the number of building blocks required in an analysis to three. However, one has to construct two sets of building blocks for determining natural frequencies and mode shapes for the two families of modes. Using the four building block scheme [8] without consideration of symmetry and antisymmetry of modes during the construction stage, only one set of four building blocks is required. The complete natural frequencies of the cantilever plate can be determined and arranged in an ascending manner. If it is desirable to identify the symmetry or antisymmetry of modes, the corresponding transcendental eigen-matrix can be modified by simply deleting rows and columns from the general eigenvalue matrix, which are disassociated with a particular family of modes of interest.

In this paper, analytical solutions for free and forced vibrations of a cantilever rectangular plate with an attached mass are obtained using the method of superposition [9] and the modal summation method [10].

To obtain an accurate analytical solution for the cantilever plate, a total of four building blocks are utilized. The superposition scheme based on the use of four building blocks is valid for arbitrary locations of attached masses. The driving quantities in the building blocks are chosen to be the bending moment for the clamped edge and the slopes taken normal to the three free edges. This choice of driving quantities eliminates the rejection modes encountered when the bending moments were chosen for free edges [9]. Although the rejection modes can be easily recovered, it is preferable not to run into the rejection modes in the first place. Numerical results are obtained using the proposed scheme are in excellent agreement with those of Gorman [9] for cantilever plates without point masses and those of Ciancio et al. [3] for plates carrying a point mass.

2. Governing differential equations

When a base motion is introduced to the clamped edge of a thin plate, the governing differential equation for lateral vibration of the plate-mass system may be written as

$$\begin{aligned} D\nabla^4 w + \rho\ddot{w} = & -m\ddot{w}\delta(x-\bar{x}, y-\bar{y}) - \rho\ddot{y}_b \\ & - m\ddot{y}_b\delta(x-\bar{x}, y-\bar{y}) - \alpha D\nabla^4\dot{w}, \end{aligned} \tag{1}$$

where $\nabla^4 = \partial^4/\partial x^4 + 2\partial^4/\partial x^2 y^2 + \partial^4/\partial y^4$; α is the structural damping coefficient; y_b is the reference lateral position of the clamped edge, measured from a space-fixed inertial coordinate frame; w is the lateral deflection of the plate, measured from the reference base position; m is the mass of the attached point mass; $\bar{x}, \bar{y}$ are the location of the point mass; $\delta(x-\bar{x}, y-\bar{y})$ is a two-dimensional Dirac delta function; D is the plate flexural rigidity, defined as $Eh^3/[12(1-v^2)]$ for a single isotropic layer of material; ρ is the plate density per unit area; x,y are the Cartesian coordinates of material points on the midplane; h is the plate thickness; E is Young's modulus of the plate material; v is the Poisson's ratio of the plate material. It should be noted that rotary inertia of the mass is not taken into account in this paper.

In the free vibration analysis of the undamped plate-mass system, the lateral displacement is assumed to vary sinusoidally with time at a natural frequency, ω_n. The amplitude of plate free vibration, normalized to the plate side length, a, is governed by the following equation:

$$D\nabla^4 W - \rho\omega_n^2 W = m\omega_n^2 W(\bar{x}, \bar{y})\delta(x-\bar{x}, y-\bar{y}). \tag{2}$$

To maximize the use of computed results, it is often desirable to work with non-dimensional quantities. Using $\xi = x/a$ and $\eta = y/b$, where a and b are the plate dimensions in the x and y directions, respectively. The preferred non-dimensional governing differential equation may be written as

$$\begin{aligned} \tilde{\nabla}^4 W - \bar{\lambda}^4 W &= P\tfrac{b}{D}\delta(\xi-\bar{\xi}, \eta-\bar{\eta}) \text{ or} \\ \tilde{\nabla}^4 W - \bar{\lambda}^4 W &= P^*\delta(\xi-\bar{\xi}, \eta-\bar{\eta}), \end{aligned} \tag{3}$$

where $P^* = Pb/D$; $P = ma\omega_n^2 W(\bar{\xi}, \bar{\eta})$; $\tilde{\nabla}^4 = \phi^2\partial^4 W/\partial\xi^4 + 2\partial^4 W/\partial\xi^2\eta^2 + \phi^{-2}\partial^4 W/\partial\eta^4$; $\bar{\lambda}^2 (= \omega_n ab\sqrt{\rho/D})$ is the non-dimensional eigenvalue parameter; ϕ $(= b/a)$ is the plate aspect ratio. The non-dimensional magnitude of the concentrated force due to the attached mass is $P^* = \mu\bar{\lambda}^4 W(\bar{\xi}, \bar{\eta})$, where μ is the ratio of the attached mass to the plate mass. The non-dimensional eigenvalue parameter introduced in this paper is slightly different from the traditional definition of $\lambda^2 = \omega_n a^2\sqrt{\rho/D}$, e.g., used by Gorman [9]. The two eigenvalue parameters are related by $\lambda^2 = \bar{\lambda}^2/\phi$. To evaluate the effect of a point mass on natural frequencies in a non-dimensional manner, the frequency parameter, $\bar{\lambda}^2$, can be used directly as a non-dimensional frequency if the plate area is fixed.

The first four building blocks do not involve the point mass. Therefore, the governing equation is further reduced to

$$\tilde{\nabla}^4 W - \bar{\lambda}^4 W = 0. \tag{4}$$

For reference, the non-dimensional bending moments and lateral edge reactions along $\xi =$ constant and $\eta =$ constant, and the non-dimensional force at any of the plate corners are related to the lateral deflection as

follows [9]:

$$-\frac{M_\xi a}{D}=\frac{\partial^2 W}{\partial\xi^2}+\nu\phi^{-2}\frac{\partial^2 W}{\partial\eta^2},\quad -\frac{M_\eta \phi b}{D}=\frac{\partial^2 W}{\partial\eta^2}+\nu\phi^{2}\frac{\partial^2 W}{\xi^2},$$
$$-\frac{V_\xi a^2}{D}=\frac{\partial^3 W}{\partial\xi^3}+\nu^*\phi^{-2}\frac{\partial^3 W}{\partial\xi\partial\eta^2},\quad -\frac{V_\eta \phi b^2}{D}=\frac{\partial^3 W}{\partial\eta^3}+\nu^*\phi^{2}\frac{\partial^3 W}{\partial\eta\partial\xi^2},\quad \frac{Rb}{2D(1-\nu)}=\frac{\partial^2 W}{\partial\xi\partial\eta},$$

where $\nu^*=2-\nu$.

3. Free vibration analysis

To obtain an analytical solution for free lateral vibration of a cantilever plate carrying a point mass, five building blocks shown in Fig. 2 are employed. The first four building blocks are required by the clamped and free edges in the cantilever plate; the fifth building block is required because of the point mass. An additional building block similar to the fifth building block is required for each additional attached mass.

Each of the first four building blocks has a driving edge and three non-driving edges. The fifth building block has a driving point corresponding to the point mass. For a non-driving edge, the boundary conditions are either simple support (represented by a dashed line beside an edge) or slip-shear (represented by a pair of small circles at the middle of an edge). For a driving edge corresponding to a free edge in the original cantilever plate, the conditions are zero lateral edge reaction and prescribed slope of plate taken normal to the edge. For a driving edge corresponding to the clamped edge in the original cantilever plate, the boundary conditions are zero lateral displacement and prescribed bending moment.

3.1. Analytical solution for the first building block

The following boundary conditions are prescribed for the first building block: simple support at edge $\xi=0$, slip-shear at edges $\eta=0$ and $\xi=1$. Along the driving edge $\eta=1$, the lateral edge reaction is set to zero, and

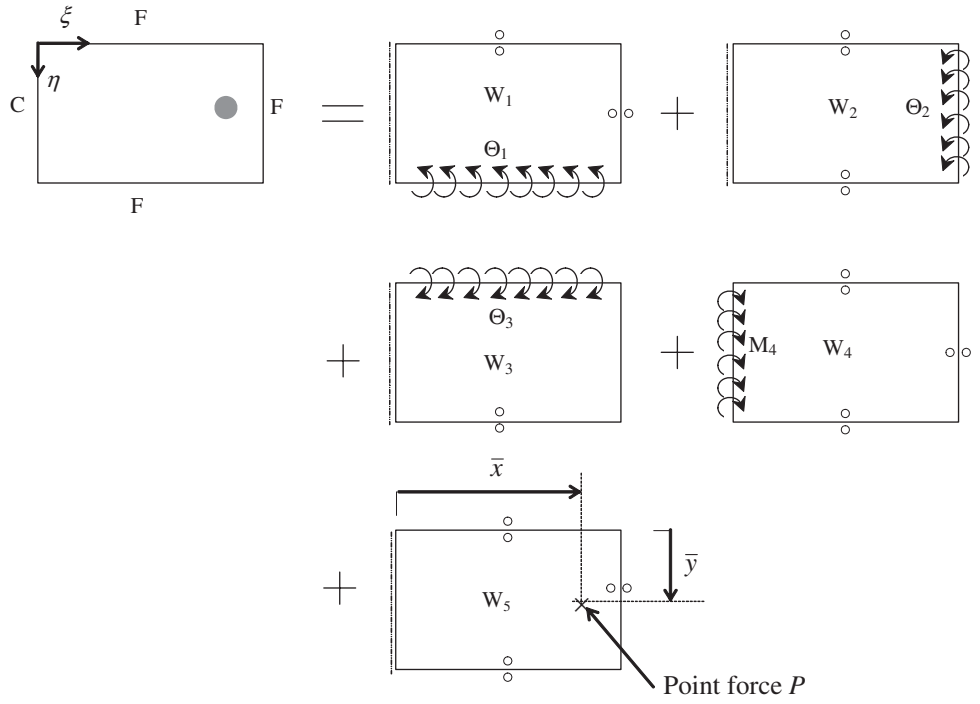

Fig. 2. Building blocks employed for obtaining an analytical solution for free vibration of a cantilever plate carrying a point mass.

the prescribed slope of plate taken normal to the edge is

$$\mathbf{\Theta}_1 = \left.\frac{\partial W_1}{\partial \eta}\right|_{\eta=1} = \sum_{m=1,2}^{K} E_{1,m} \sin \bar{m}\pi\xi, \tag{5}$$

where $E_{1,m}$ is a set of unknown coefficients, which determine the distribution of slope along $\eta = 1$ for a vibration mode. Values of these coefficients can be determined when a solution to the original problem is obtained.

A Levy type solution for this building may be written as

$$W_1 = \sum_{m=1,2}^{K} Y_m(\eta) \sin \bar{m}\pi\xi, \tag{6}$$

where $\bar{m} = (2m-1)/2$ and K is the number of terms employed in the series solution.

Substituting Eq. (6) into Eq. (4), one obtains the following ordinary differential equation:

$$Y_m''' - 2(\phi\bar{m}\pi)^2 Y_m'' + \left((\phi\bar{m}\pi)^4 - \phi^2\bar{\lambda}^4\right) Y_m = 0. \tag{7}$$

An exact solution to the above equation may be written in the following form:

$$Y_m = A_m \cosh(\beta_m\eta) + B_m \sinh(\beta_m\eta) + C_m \mathrm{cs}(\gamma_m\eta) + D_m \mathrm{sn}(\gamma_m\eta), \tag{8}$$

where $\beta_m = \sqrt{(\phi\bar{m}\pi)^2 + \phi\bar{\lambda}^2}$, $\gamma_m = \sqrt{(\phi\bar{m}\pi)^2 - \phi\bar{\lambda}^2}$ or $\gamma_m = \sqrt{\phi\bar{\lambda}^2 - (\phi\bar{m}\pi)^2}$, whichever is real; A_m, B_m, C_m and D_m are unknown constants to be determined from the boundary conditions. Functions $\mathrm{cs}(\gamma_m\eta)$ and $\mathrm{sn}(\gamma_m\eta)$ are defined as follows:

$$\mathrm{cs}(\gamma_m\eta) = \begin{cases} \cos(\gamma_m\eta) & \text{if } (\bar{m}\pi)^2 < \bar{\lambda}^2/\phi, \\ \cosh(\gamma_m\eta) & \text{if } (\bar{m}\pi)^2 > \bar{\lambda}^2/\phi. \end{cases}$$

$$\mathrm{sn}(\gamma_m\eta) = \begin{cases} \sin(\gamma_m\eta) & \text{if } (\bar{m}\pi)^2 < \bar{\lambda}^2/\phi, \\ \sinh(\gamma_m\eta) & \text{if } (\bar{m}\pi)^2 > \bar{\lambda}^2/\phi. \end{cases}$$

Enforcing the boundary conditions on edge $\eta = 0$, one finds that the unknown coefficients B_m and D_m are zero. The number of unknowns is consequently reduced to two. From the remaining conditions along the driving edge $\eta = 1$, one may find the other two unknowns. The analytical solution for the first building block is

$$W_1 = \sum_{m=1,2}^{K} E_{1,m}\left(\theta_{11,m}\frac{\cosh(\beta_m\eta)}{\sinh\ \beta_m} + \theta_{13,m}\frac{\mathrm{cs}(\gamma_m\eta)}{\mathrm{sn}\gamma_m}\right) \sin \bar{m}\pi\xi, \tag{9}$$

where $\theta_{11,m} = -\gamma_m^2 - [\pm\nu^*(\phi\bar{m}\pi)^2]/\beta_m[\pm\beta_m^2 - \gamma_m^2]$; $\theta_{13,m} = \beta_m^2 - \nu^*(\phi\bar{m}\pi)^2/\gamma_m[\pm\beta_m^2 - \gamma_m^2]$. The minus sign here and in the solution for the third building block applies if $(\bar{m}\pi)^2 < \bar{\lambda}^2/\phi$.

3.2. Analytical solution for the second building block

The second building block has a pair of slip shear edges along $\eta = 0$ and 1, and a simply supported edge along $\xi = 0$. The conditions along the driving edge $\xi = 1$ are zero lateral reaction and prescribed angle of rotation, given by

$$\mathbf{\Theta}_2 = \left.\frac{\partial W_2}{\partial \xi}\right|_{\xi=1} = \sum_{n=0,1}^{K-1} E_{2,n} \cos n\pi\eta. \tag{10}$$

A Levy solution for the second building block may be written as

$$W_2 = \sum_{n=0,1}^{K-1} Y_n(\xi)\cos\, n\pi\eta. \tag{11}$$

For convenience, the number of terms in the Levy solution is set to be the same as in that for the first building block. It is noted that, when dealing with very small or very large plate aspect ratios, it may be beneficial to use different number of terms in different building blocks in order to reduce the computations while maintaining good accuracy [9].

Following the procedure similar to that used for the first building block, one obtains the following analytical solution:

$$W_2 = \sum_{n=0,1}^{K-1} E_{2,n}\left[\theta_{22,n}\frac{\sinh(\beta_n\xi)}{\cosh\,\beta_n} + \theta_{24,n}\frac{\mathrm{sn}(\gamma_n\xi)}{\mathrm{cs}\,\gamma_n}\right]\cos\, n\pi\eta, \tag{12}$$

where $\beta_n = \sqrt{(n\pi/\phi)^2 + \bar{\lambda}^2/\phi}$, $\gamma_n = \sqrt{(n\pi/\phi)^2 - \bar{\lambda}^2/\phi}$ or $\gamma_n = \sqrt{\bar{\lambda}^2/\phi - (n\pi/\phi)^2}$, whichever is real, and

$$\mathrm{cs}(\gamma_n\xi) = \begin{cases} \cos(\gamma_n\xi) & \text{if } (n\pi)^2 < \bar{\lambda}^2\phi, \\ \cosh(\gamma_n\xi) & \text{if } (n\pi)^2 > \bar{\lambda}^2\phi. \end{cases}$$

$$\mathrm{sn}(\gamma_n\xi) = \begin{cases} \sin(\gamma_n\xi) & \text{if } (n\pi)^2 < \bar{\lambda}^2\phi, \\ \sinh(\gamma_n\xi) & \text{if } (n\pi)^2 > \bar{\lambda}^2\phi. \end{cases}$$

$$\theta_{22,n} = -\frac{\pm\gamma_n^2 - \nu^*(n\pi/\phi)^2}{\beta_n[\beta_n^2 - (\pm\gamma_n^2)]}, \quad \theta_{24,n} = -\frac{\beta_n^2 - \nu^*(n\pi/\phi)^2}{\gamma_n[\beta_n^2 - (\pm\gamma_n^2)]}.$$

In the above equations and in the solution for the fourth building, the minus sign applies if $(n\pi)^2 < \bar{\lambda}^2\phi$.

3.3. Analytical solution for the third building block

The third building block has the same boundary conditions at $\xi = 0$ and 1 as those in the first building. It has slip-shear boundary conditions at $\eta = 1$ and zero lateral reaction at $\eta = 0$. Along the driving edge $\eta = 0$, the lateral edge reaction is zero; the slope taken normal the edge is prescribed to be

$$\Theta_3 = \left.\frac{\partial W_3}{\partial\eta^*}\right|_{\eta^*=1} = \sum_{m=1,2}^{K} E_{3m}\sin\,\bar{m}\pi\xi, \tag{13}$$

where $\eta^* = 1-\eta$.

Comparing the first and the third building blocks, one finds that the only difference is the swap of the boundary conditions at $\eta = 0$ and 1. As a result, the analytical solution for the third building may be inferred from that for the first building. For completeness, the analytical solution for the third building block is given below

$$W_3 = \sum_{m=1,2}^{K} E_{3,m}\left(\theta_{11,m}\frac{\cosh(\beta_m\eta^*)}{\sinh\,\beta_m} + \theta_{13,m}\frac{\mathrm{cs}(\gamma_m\eta^*)}{\mathrm{sn}\,\gamma_m}\right)\sin\,\bar{m}\pi\xi. \tag{14}$$

3.4. Analytical solution for the fourth building block

The fourth building block has the three slip shear edges along edges at $\eta = 0$, $\eta = 1$, and $\xi = 1$. The condition along the driving edge $\xi = 0$ are zero displacement and the following prescribed bending moment

$$M_4 = \left.\frac{M_{\xi^*}a}{D}\right|_{\xi^*=1} = \sum_{n=0,1}^{k-1} E_{4,n}\cos\, n\pi\eta, \tag{15}$$

where $\xi^* = 1-\xi$.

To obtain an analytical solution in the most compact form, an analytical solution for this building block is written as follows:

$$W_4 = \sum_{n=0,1}^{k-1} \bar{Y}_n(\xi^*) \cos n\pi\eta. \tag{16}$$

The analytical solution for $\bar{Y}_n(\xi^*)$ may be obtained in a manner similar to that used for the second building block. For reference and completeness, the solution is presented below

$$W_4 = \sum_{n=0,1}^{k-1} E_{4,n} \left[\theta_{41,n} \frac{\cosh(\beta_n \xi^*)}{\cosh\ \beta_n} + \theta_{43,n} \frac{\mathrm{cs}(\gamma_n \xi^*)}{\mathrm{cs}\,\gamma_n} \right] \cos n\pi\eta, \tag{17}$$

where β_n and γ_n are identical to those appearing in the solution for the second building block. Other parameters are $\theta_{41n} = 1/(-\beta_n^2 \pm \gamma_n^2), \theta_{43n} = -1/(\beta_n^2 \pm \gamma_n^2)$.

3.5. Analytical solution for the fifth building block

The fifth building block has one simply supported edge and three slip-shear edges. It is subjected to a concentrated force at the location of the attached point mass. An exact Navier solution to Eq. (3) for this building block may be written as

$$W_5(\xi, \eta) = \sum_{m=1,2}^{k} \sum_{n=0,1}^{k-1} a_{mn} \sin \bar{m}\pi\xi \cos n\pi\eta. \tag{18}$$

The above solution satisfies the boundary condition along all four edges. To obtain a solution to Eq. (3), the Dirac delta function, $\delta(\xi - \bar{\xi}, \eta - \bar{\eta})$, on the right-hand side of the equation needs to be expanded into the double Fourier series. Utilizing the orthogonality conditions for functions $\sin \bar{m}\pi\xi \cos n\pi\eta$ in domain $0 \leqslant \xi \leqslant 1$ and $0 \leqslant \eta \leqslant 1$, the Fourier series coefficients may be obtained. The Dirac delta function may be expressed as

$$\delta(\xi - \bar{\xi}, \eta - \bar{\eta}) = \sum_{m=1,2}^{k} \sum_{n=0,1}^{k-1} 2\alpha_n \sin \bar{m}\pi\bar{\xi} \cos n\pi\bar{\eta} \sin \bar{m}\pi\xi \cos n\pi\eta, \tag{19}$$

where α_n is 1 for $n = 0$ and 2 for $n \neq 0$.

Substituting Eq. (19) into Eq. (3), the analytical solution for the fifth building block is

$$W_5 = P^* \sum_{m=1,2}^{k} \sum_{n=0,1}^{k-1} a'_{mn} \sin \bar{m}\pi\xi \cos n\pi\eta, \tag{20}$$

where $a'_{mn} = 2\alpha_n \sin \bar{m}\pi\bar{\xi} \cos n\pi\bar{\eta} / \phi^2 \left[(\bar{m}\pi)^2 + (n\pi/\phi)^2 \right]^2 - \bar{\lambda}^4$.

3.6. Analytical solution for a cantilever plate with an attached mass

Now the analytical solutions for all building blocks are available. To obtain a solution for the cantilever plate carrying a point mass, the solutions for all individual building blocks are superimposed in the following manner:

$$W(\xi, \eta) = \sum_{j=1}^{5} W_j(\xi, \eta). \tag{21}$$

Since the governing equations are linear, the superimposed solution satisfies the same governing differential equation. It also satisfies one of the two boundary conditions along each of the four edges. The superimposed solution in Eq. (21) contains a total of $4k + 1$ unknown constants. In order for the superimposed solution to be the solution for the original problem, it must satisfy the remaining boundary condition along each edge. By doing so, all unknowns in the superimposed solution can be determined.

Starting from edge $\eta = 1$, the boundary conditions for the four edges of a cantilever are free, free, free and clamped in a counterclockwise manner. For a free edge, the lateral reaction force is already zero along the corresponding edge in each block. It is only necessary to enforce the zero bending moment along the three free edges. For the clamped edge, the displacement is already zero along the corresponding edge in each building block. Only the slope taken normal to the clamped edge is required to be zero. The four boundary conditions to be satisfied are

$$\left(\frac{\partial^2}{\partial\eta^2}+\nu\phi^2\frac{\partial^2}{\xi^2}\right)\left(\sum_{j=1}^{5}W_j\right)_{\eta=1}=0,\quad \left(\frac{\partial^2}{\partial\xi^2}+\nu\phi^{-2}\frac{\partial^2}{\partial\eta^2}\right)\left(\sum_{j=1}^{5}W_j\right)_{\xi=1}=0,$$
$$\left(\frac{\partial^2}{\partial\eta^2}+\nu\phi^2\frac{\partial^2}{\xi^2}\right)\left(\sum_{j=1}^{5}W_j\right)_{\eta=0}=0,\quad \frac{\partial}{\partial\xi}\left(\sum_{j=1}^{5}W_j\right)_{\xi=0}=0. \tag{22}$$

To ensure that the conditions in Eq. (22) are satisfied everywhere along edges $\eta = 0$ and $\eta = 1$, all functions in the bending moment expressions are expanded into Fourier sine series, $\sin \bar{m}\pi\xi$, in interval [0,1]; the Fourier series coefficients for each $\bar{m}$ are subsequently set to zero. As a result, the first and third condition each yields k algebraic equations. Similarly, to ensure that the conditions in Eq. (22) are satisfied everywhere along edges $\xi = 1$ and $\xi = 0$, all functions in the bending moment and slope expressions are expanded into Fourier cosine series, $\cos n\pi\eta$, in interval [0,1]; enforcement of all Fourier coefficients to be zero yields another $2k$ algebraic equations.

The solution for the fifth building block in Eq. (20) is valid for arbitrary point load. In the case of the attached point mass, the point load is caused by the inertial force of the point mass. The magnitude of this force is defined as

$$P = ma\omega_n^2\sum_{j=1}^{5}W_j(\bar{\xi},\bar{\eta}). \tag{23}$$

Dividing both sides of Eq. (23) and expressing P in terms P^*, one obtains the following additional condition due to a point mass:

$$\mu\bar{\lambda}^4\sum_{j=1}^{4}W_j(\bar{\xi},\bar{\eta})+P^*\left[\left(\mu\bar{\lambda}^4\sum_{m=1,2}^{k}\sum_{n=0,1}^{k-1}a'_{mn}\sin\bar{m}\pi\bar{\xi}\cos n\pi\bar{\eta}\right)-1\right]=0. \tag{24}$$

For a cantilever plate, there are two free corners at (1, 0) and (1, 1). To ensure that equilibrium conditions hold at the two free corners, the corner force R at the two free corners must vanish. An examination of the superimposed solution indicates that the non-dimensional corner force $\partial^2 W/\partial\xi\partial\eta$ indeed vanishes at the two free corners.

Enforcing conditions in Eqs. (22) and (24), one obtains the following $4k+1$ homogeneous algebraic equations for $4k+1$ unknowns:

$$\mathbf{\Omega x} = \mathbf{0}, \tag{25}$$

where $\mathbf{\Omega}$ is the coefficient matrix, whose elements are defined in Appendix A; $\mathbf{x}$ is the eigenvector consisting of $4k+1$ unknown constants in the analytical solution.

The condition for a non-trivial solution is that the determinant of matrix $[\mathbf{\Omega}]$ must vanish. This yields a single transcendental equation for determining the eigenvalues of free vibration of cantilever plates having an attached mass. Once zero roots of the transcendental equation or eigenvalues are obtained, the mode shapes can then be determined by solving the algebraic equations and the analytical solutions for the five building blocks.

Two test cases were selected for convergence and accuracy tests. The first test case involves a cantilever plate without attached mass, for which an analytical solution is available in the literature [7]. Numerical results in Table 1 depict that the computed eigenvalues converge to the accurate values very rapidly for the first six vibration modes. The second test case involves cantilever plates of different aspect ratios with an attached mass at (1.0, 0.5), for which results are reported in Ref. [3]. When a point mass is added, the convergence rate

Table 1
Convergence tests and verifications of computed eigenvalues for a cantilever plate without attached mass

K	Modes					
	1	2	3	4	5	6
8	3.468	7.116	18.18	22.21	27.59	42.76
10	3.469	7.116	18.18	22.21	27.58	42.76
12	3.469	7.115	18.18	22.21	27.58	42.76
14	3.469	7.115	18.18	22.21	27.58	42.76
Gorman [9]	3.470	7.115	18.18	22.21	27.58	42.76

$\lambda^2 = \omega_n a^2 \sqrt{\rho h/D}$, $\phi = 1.25$, $V = 0.333$.

Table 2
Comparisons of computed eigenvalues for symmetric modes of cantilever plates carrying a point mass

Modes	$\phi = 0.5$		$\phi = 1.0$		$\phi = 2.0$	
	Current	Ref. [3]	Current	Ref. [3]	Current	Ref. [3]
1	1.964	1.963	1.962	1.961	1.886	1.885
2	16.08	16.06	13.72	13.71	7.218	7.215
3	45.96	45.88	25.71	25.71	17.36	17.34
4	78.83	78.80	41.03	40.99	24.09	24.09
5	105.5	105.4	59.92	59.92	33.83	33.83

$\lambda^2 = \omega_n a^2 \sqrt{\rho h/D}$, $\bar{\xi} = 1.0, \bar{\eta} = 0.5$, $\mu = 0.5$, $V = 0.3$, $K = 20$.

is slightly slower. As a result, 20 terms are used in the Levy solutions. It can be seen from Table 2 that there is excellent agreement in computed eigenvalues between the current work and those of Ref. [3].

3.7. Mode shapes for a cantilever plate with an attached mass

To handle the response of a cantilever plate carrying a point mass under the base excitation, the modal summation method is used. For this reason, the orthogonality conditions of mode shapes of undamped plate free vibration and their orthogonality relations are discussed here.

Assume that a set of M eigenvalues, $\bar{\lambda}_i^2$ or $\omega_{n,i}$, and their corresponding mode shapes, ϕ_i, $i = 1,2,\ldots M$, are determined and arranged in an ascending manner. The i-th and j-th mode shape functions satisfy the following equations:

$$\begin{aligned} D\nabla^4\phi_i &= \rho\omega_{n,i}^2\phi_i + m\omega_{n,i}^2\phi_i\delta(x-\bar{x},y-\bar{y}),\\ D\nabla^4\phi_j &= \rho\omega_{n,j}^2\phi_j + m\omega_{n,j}^2\phi_j\delta(x-\bar{x},y-\bar{y}). \end{aligned} \tag{26}$$

Invoking the reciprocal theorem [10], one finds that, for a plate having homogenous classical boundary conditions, the following orthogonal conditions hold:

$$\begin{aligned} &\int_A \rho\phi_i\phi_j \,\mathrm{d}A + m\phi_i(\bar{x},\bar{y})\phi_j(\bar{x},\bar{y}) = m_j\delta_{ij},\\ &\int_A D\phi_i\nabla^4\phi_j \,\mathrm{d}A = m_j\omega_{n,j}^2\delta_{ij}, \end{aligned} \tag{27}$$

where m_i is the i-th modal mass; δ_{ij} is the Kronecker delta. The above orthogonality condition pairs may be written in the following non-dimensional form

$$\int_0^1\int_0^1 \phi_i\phi_j \,\mathrm{d}\xi \,\mathrm{d}\eta + \mu\phi_i(\bar{\xi},\bar{\eta})\phi_j(\bar{\xi},\bar{\eta}) = \mu_j\delta_{ij}, \tag{28}$$

$$\int_0^1 \int_0^1 \phi_i \tilde{\nabla}^4 \phi_j \, \mathrm{d}\xi \, \mathrm{d}\eta = \mu_j \bar{\lambda}_j^4 \delta_{ij},$$

where μ_j is the ratio of the modal mass to the plate mass, defined as $m_j/\rho ab$.

4. Forced vibration due to harmonic base motion

To determine the response of the cantilever plate with a point mass under the excitation of the harmonic base motion, $y_b = Y_b \sin \omega t$, the modal summation method is employed. A solution to Eq. (1) is sought in the following manner:

$$w(x, y, t) = \sum_{j=1}^{M} \phi_j(\xi, \eta) g_j(\tau), \tag{29}$$

where τ is the non-dimensional time, defined as $\tau = \omega_{n,1} t$.

Substituting Eq. (29) into Eq. (1), multiplying both sides of the so-obtained equation by $\Phi_i(\xi,\eta)$, and integrating over the entire plate area, one obtains

$$g_i'' + 2\zeta_i r_i g_i' + r_i^2 g_i = \chi_i r^2 Y_b \sin r\tau, \tag{30}$$

where $r = \omega/\omega_{n,1}$; $r_i = \omega_{n,i}/\omega_{n,1}$; $\zeta_i = \alpha\omega_{n,i}/2$; χ_i is the modal participation factor, defined as

$$\chi_i = \frac{1}{\mu_i}\left[\int_0^1 \int_0^1 \phi_i \, \mathrm{d}\xi \, \mathrm{d}\eta + \mu\phi_i(\bar{\xi}, \bar{\eta})\right] = \frac{\int_0^1 \int_0^1 \phi_i \, \mathrm{d}\xi \, \mathrm{d}\eta + \mu\phi_i(\bar{\xi}, \bar{\eta})}{\int_0^1 \int_0^1 \phi_i^2 \, \mathrm{d}\xi \, \mathrm{d}\eta + \mu\phi_i^2(\bar{\xi}, \bar{\eta})}. \tag{31}$$

The normalized steady state response amplitude of the i-th modal coordinate is

$$\frac{G_i}{Y_b} = \underbrace{\frac{r^2}{\sqrt{(r_i^2 - r^2)^2 + (2\zeta_i r_i r)^2}}}_{\text{dynamic factor}} \underbrace{\chi_i}_{\text{modal participation factor}} \tag{32}$$

For a given source of motion, there are two factors influencing the system response. They are the dynamical factor and the modal participation factor. To maximize the fundamental response amplitude, the non-dimensional excitation frequency should be tuned to be in the vicinity of unity. However, this tuning does not eliminate participation of higher vibration modes. Participation of the i-th vibration mode is determined by χ_i.

An examination of Eq. (31) reveals that for a cantilever plate, the entire family of vibration modes, antisymmetric with respect to the major centerline or $\bar{\eta} = 0.5$, will be completely eliminated from participations in the response if the mass is attached along the major centerline. Only the vibration modes, which are symmetric with respect to the major centerline, are participating in the response. With the mass attached along $\bar{\eta} = 0.5$, it is only necessary to deal with three non-dimensional parameters, $\bar{\xi}$, μ, and ϕ. It is not possible to tabulate or graph the effects of the three non-dimensional parameters on the eigenvalues and the modal participation factors. In this paper, the numerical results are presented for $\phi = 0.5$ and 1.0, $\nu = 0.3$, and $\mu = 0.1$, 0.5, and 1.0. As for the location of the attached mass, parameter $\bar{\xi}$ is considered to vary in a fine increment in the interval [0,1].

The eigenvalues of the first two symmetric modes for square plates carrying point masses were obtained and presented in Fig. 3. For each of the three mass ratios, the first symmetric eigenvalue remains almost unchanged if the mass is attached near the clamped edge. However, if the mass is placed away from the clamped edge, the fundamental eigenvalue decreases considerably with increasing distance until the free edge as shown in Fig. 3a. At the free edge, the fundamental eigenvalue reaches its minimum value for a specified mass ratio. The maximum percentage decreases are 16.0% for $\mu = 0.1$, 43.5% for $\mu = 0.5$, and 56.0% for $\mu = 1.0$. For the second symmetric mode, the eigenvalues vary with the distance from the clamped edge in a waveform. This is because the second symmetric mode of the square cantilever plate without an attached mass has a nodal line crossing the major centerline at $\xi = 0.74$. The displacements on the two sides of the nodal line are out of phase. If the mass is placed at the nodal line, it has no effect on the eigenvalue. On the other hand, if it is

placed near an antinode or the maximum modal displacement point, its effect on the eigenvalues is most significant. An examination of modal contours reveals that the nodal line never passes through the location of the attached mass. In other words, the point mass cannot be located at a node line. The closest distance between the nodal line and the location of the attachment is achieved if the point mass is at $\xi = 0.74$.

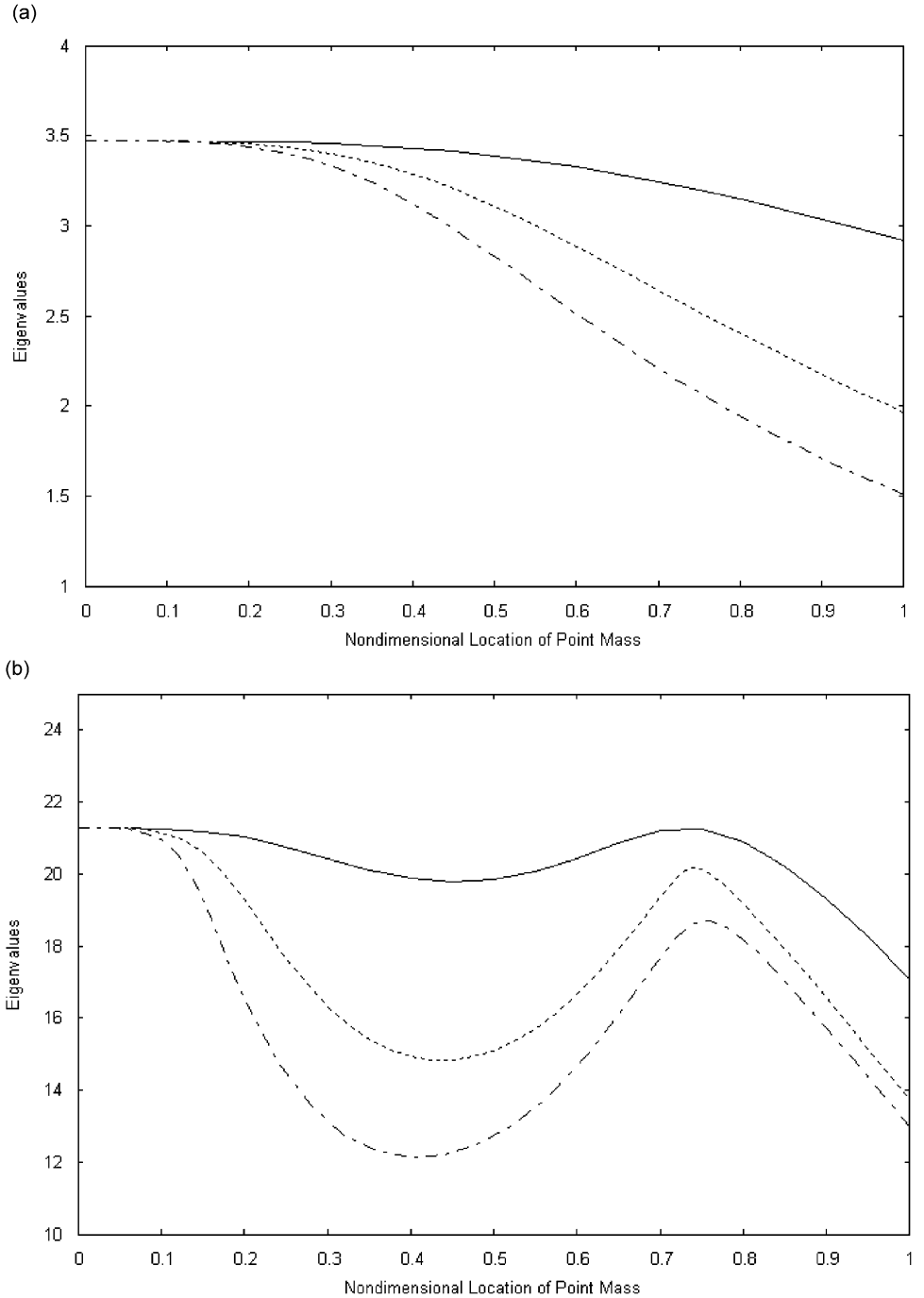

Fig. 3. Variation of eigenvalues of square cantilever plates with the location of the attachment along $\eta = 0.5$ for different mass ratios: (a) first symmetric mode (mass ratio 0.1 —, mass ratio 0.5 – – – –, mass ratio 1.0 — – —); (b) second symmetric mode (mass ratio 0.1 —, mass ratio 0.5 – – – –, mass ratio 1.0 — – —).

As shown in Fig. 3b, the eigenvalue reaches a maximum at this location, which shifts gradually outward with increasing mass ratios. Modal participation factors for the first two symmetric modes of a cantilever square plate are shown in Fig. 4 for three different mass ratios and a range of non-dimensional locations along the major axis. From the view point of increasing participation of the fundamental mode in the response, it is

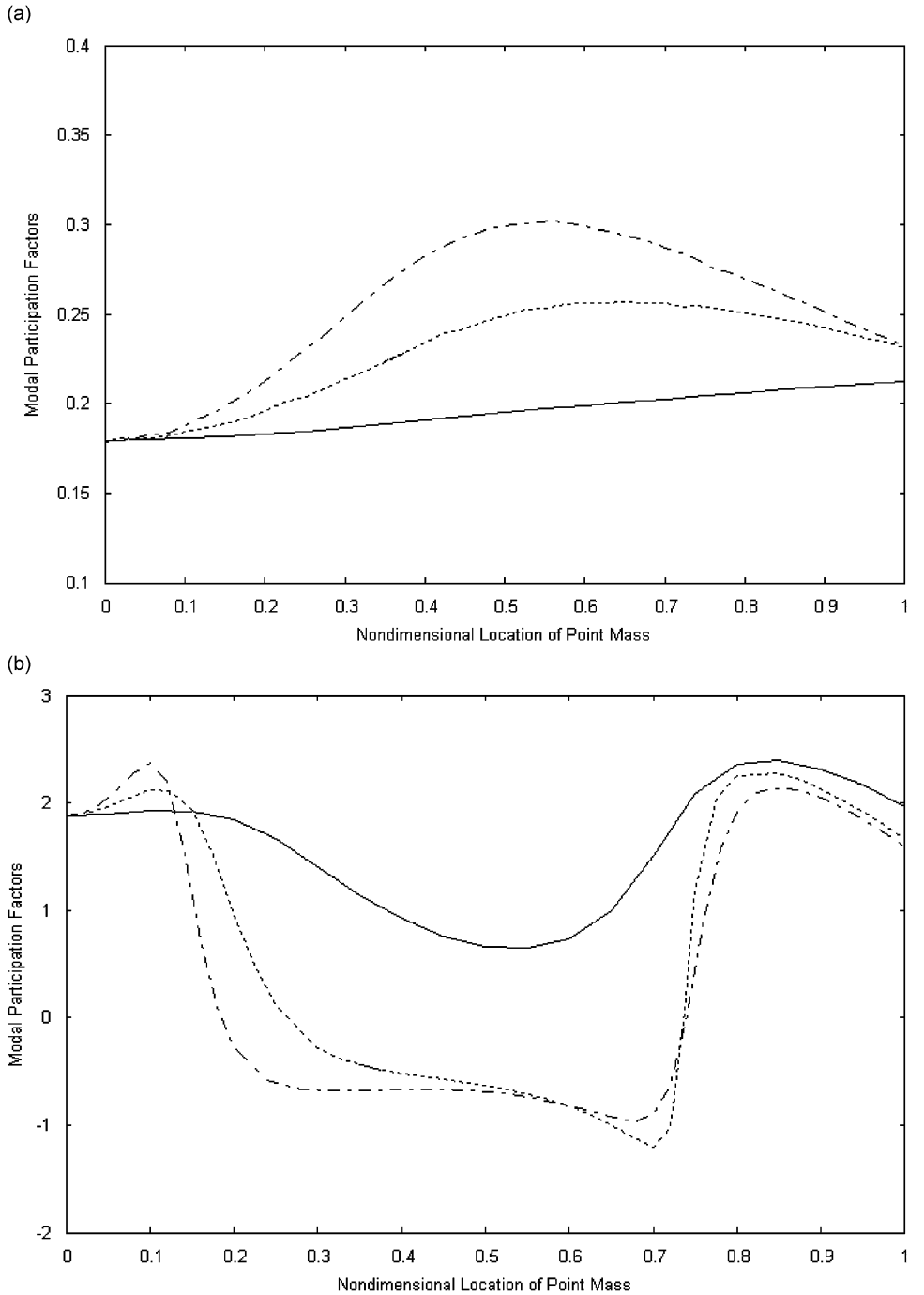

Fig. 4. Variation of modal participation factors of square cantilever plates with the location of the attachment for different mass ratios: (a) first symmetric mode (mass ratio 0.1 —, mass ratio 0.5 – – – –, mass ratio 1.0 — – —); (b) second symmetric mode (mass ratio 0.1 —, mass ratio 0.5 – – – –, mass ratio 1.0 — – —).

beneficial to use larger mass and have it attached slightly beyond the midpoint of the major centerline. However, to reduce or eliminate the participation of the second symmetric mode, one ideal location is $\xi = 0.74$. At this location, the modal participation factors for the second symmetric mode are zero for $\mu = 0.5$ and 1.0. However, for small mass ratio, the zero second modal participation is not expected. This is because

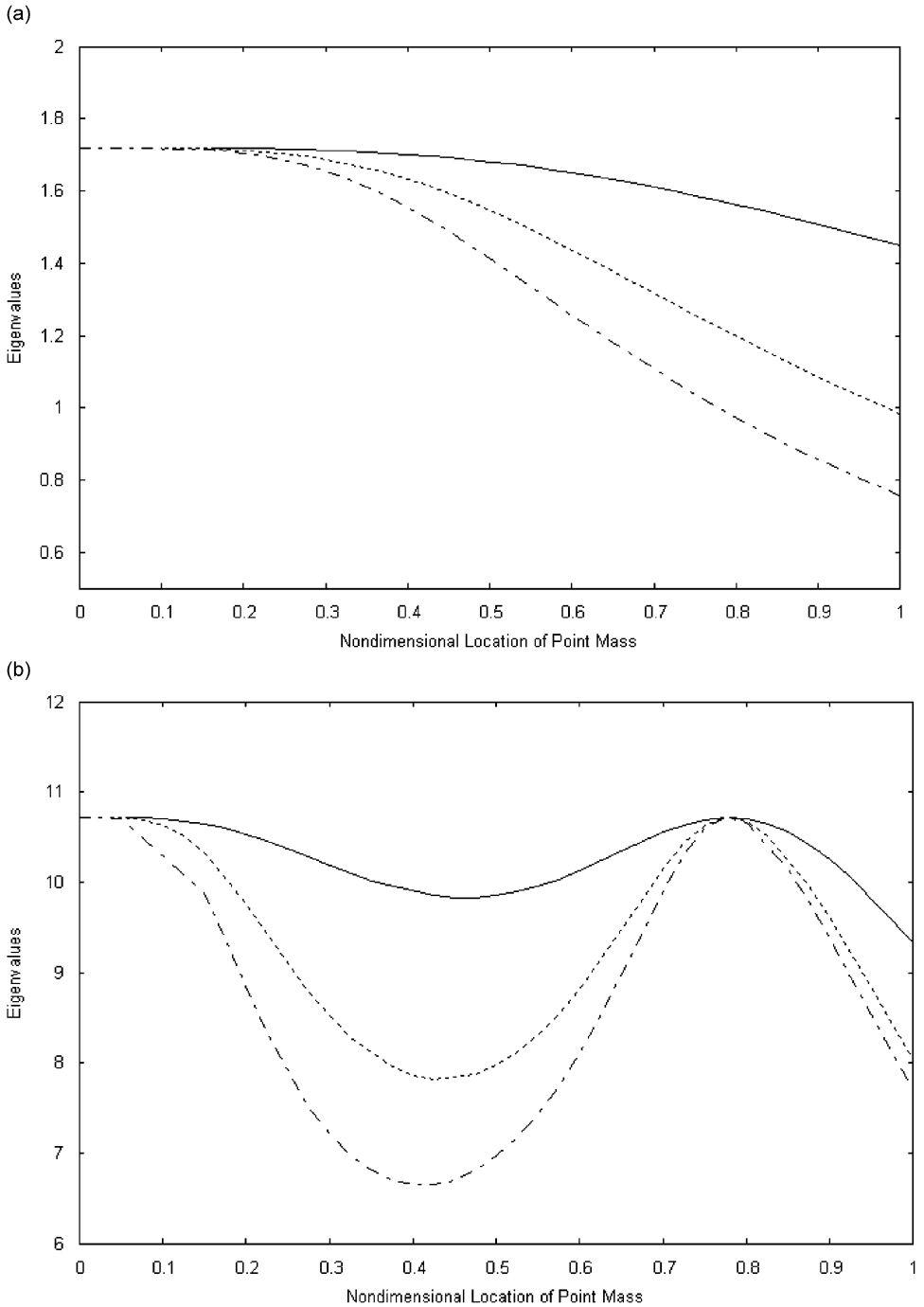

Fig. 5. Variation of eigenvalues of rectangular cantilever plates ($\phi = 0.5$) with the location of the attachment along $\eta = 0.5$ for different mass ratios: (a) first symmetric mode (mass ratio 0.1 —, mass ratio 0.5 – – – –, mass ratio 1.0 — – —); (b) second symmetric mode (mass ratio 0.1 —, mass ratio 0.5 – – – –, mass ratio 1.0 — – —).

small point mass does not significantly alter the shape of the second symmetric mode of a square cantilever plate. In typical applications, the attached mass is usually many times the mass of the base plate in order to harvest vibrational energy of low frequency.

For cantilever rectangular plates of $\phi = 0.5$, the eigenvalues are presented in Fig. 5 for $\mu = 0.1$, 0.5, 1.0 and a range of non-dimensional location parameter. It can be seen that the natural frequencies of symmetric modes of the rectangular plates are significantly lower than those for the square plates. The eigenvalues of the first symmetric modes decrease steadily with both the mass ratio and the non-dimensional distance of the attached mass from the clamped edge. This wide range of monotonic variation in the natural frequency provides a reliable way for designing the fundamental natural frequency in accordance with the source frequency. For the second symmetric modes, the eigenvalues vary in a waveform. At $\xi = 0.775$, the eigenvalues are not affected by the attached mass. Attachment of a point mass to this location along the major centerline tends to maximize the participation of the first symmetric mode and minimize the participation of the second symmetric mode in the steady state response due to base motion.

5. Conclusions

Analytical solutions for free and forced vibrations of cantilever square and rectangular plates carrying single attached masses are obtained in this paper using Gorman's method of superposition and the modal summation method. Comparisons with the previously published results indicate that the procedure presented in this paper is accurate and convergent. Results presented in this paper are useful in designing frequencies and modal participations for piezoelectric structures in the area of power generation.

Appendix A

Non-zero elements of matrix $\mathbf{\Omega}$ in Eq. (25) are given below, where indices $m = 1, 2, \ldots, k$; $n = 0, 1, 2, \ldots k-1$; k is the number of terms used in the Levy solutions for all building blocks.

$$\mathbf{\Omega}(m,m) = \theta_{11,m}[\beta_m^2 - v(\phi\bar{m}\pi)^2]\frac{\cosh\,\beta_m}{\sinh\,\beta_m} + \theta_{13,m}[\pm\gamma_m^2 - v(\phi\bar{m}\pi)^2]\frac{\mathrm{cs}\,\gamma_m}{\mathrm{sn}\,\gamma_m}. \tag{A.1}$$

$$\mathbf{\Omega}(m,k+n+1) = \theta_{22,n}I_{1,mn}[v\phi^2\beta_m^2 - (n\pi)^2]\cos\,n\pi + \theta_{24,n}I_{2,mn}[\pm v\phi^2\gamma_m^2 - (n\pi)^2]\cos\,n\pi. \tag{A.2}$$

$$\mathbf{\Omega}(m,2k+m) = \theta_{11,m}[\beta_m^2 - v(\phi\bar{m}\pi)^2]\frac{1}{\sinh\,\beta_m} + \theta_{13,m}[\pm\gamma_m^2 - v(\phi\bar{m}\pi)^2]\frac{1}{\mathrm{sn}\,\gamma_m}. \tag{A.3}$$

$$\mathbf{\Omega}(m,3k+n+1) = \theta_{41,n}I_{3,mn}[v\phi^2\beta_m^2 - (n\pi)^2]\cos\,n\pi + \theta_{43,n}I_{4,mn}[\pm v\phi^2\gamma_m^2 - (n\pi)^2]\cos\,n\pi. \tag{A.4}$$

$$\mathbf{\Omega}(3k+n+1,m) = \theta_{11,m}I_{5,nm}[v\beta_m^2\phi^{-2} - (\bar{m}\pi)^2] + \theta_{13,m}I_{6,nm}[\pm v\gamma_m^2\phi^{-2} - (\bar{m}\pi)^2]. \tag{A.5}$$

$$\mathbf{\Omega}(3k+n+1,k+n+1) = \theta_{22,n}[\beta_n^2 - v(n\pi/\phi)^2]\frac{\sinh\,\beta_n}{\cosh\,\beta_n} + \theta_{24,n}[\pm\gamma_m^2 - v(n\pi/\phi)^2]\frac{\mathrm{sn}\,\gamma_n}{\mathrm{cs}\,\gamma_n}. \tag{A.6}$$

$$\mathbf{\Omega}(3k+n+1,2k+m) = \theta_{11,m}I_{7,nm}[v\beta_m^2\phi^{-2} - (\bar{m}\pi)^2] + \theta_{13,m}I_{8,nm}[\pm v\gamma_m^2\phi^{-2} - (\bar{m}\pi)^2]. \tag{A.7}$$

$$\mathbf{\Omega}(3k+n+1,3k+n+1) = \theta_{41,n}[\beta_n^2 - v(n\pi/\phi)^2]\frac{1}{\cosh\,\beta_n} + \theta_{43,n}[\pm\gamma_m^2 - v(n\pi/\phi)^2]\frac{1}{\mathrm{cs}\,\gamma_n}. \tag{A.8}$$

$$\mathbf{\Omega}(2k+m,m) = \mathbf{\Omega}(m,2k+m). \tag{A.9}$$

$$\mathbf{\Omega}(2k+m,k+n+1) = \mathbf{\Omega}(m,k+n+1)/\cos(n\pi). \tag{A.10}$$

$$\begin{aligned}&\mathbf{\Omega}(2k+m,2k+m) = \mathbf{\Omega}(m,m),\\ &\mathbf{\Omega}(2k+m,3k+n+1) = \mathbf{\Omega}(m,3k+n+1)/\cos(n\pi).\end{aligned} \tag{A.11}$$

$$\mathbf{\Omega}(3k+n+1,m)=\theta_{11,m}\imath\bar{m}\pi I_{5,nm}+\theta_{13,m}\imath\bar{m}\pi I_{6,nm}. \tag{A.12}$$

$$\mathbf{\Omega}(3k+n+1,k+n+1)=\theta_{22,n}\beta_n\frac{1}{\cosh\,\beta_n}+\theta_{24,n}\gamma_n\frac{1}{\mathrm{cs}\,\gamma_n}. \tag{A.13}$$

$$\mathbf{\Omega}(3k+n+1,2k+m)=\theta_{11,m}I_{7,nm}\imath\bar{m}\pi+\theta_{13,m}I_{8,nm}\imath\bar{m}\pi. \tag{A.14}$$

$$\mathbf{\Omega}(3k+n+1,3k+n+1)=-\theta_{41,n}\beta_n\frac{\sinh\,\beta_n}{\cosh\,\beta_n}-\theta_{43,n}(\pm\gamma_n)\frac{\mathrm{sn}\,\gamma_n}{\mathrm{cs}\,\gamma_n}. \tag{A.15}$$

$$\mathbf{\Omega}(4k+1,m)=\mu^2\bar{\lambda}^4\left[\theta_{11,m}\frac{\cosh(\beta_m\bar{\eta})}{\sinh\,\beta_m}+\theta_{13,m}\frac{\mathrm{cs}(\gamma_m\bar{\eta})}{\mathrm{sn}\,\gamma_m}\right]\sin\,\imath\bar{m}\pi\bar{\xi}. \tag{A.16}$$

$$\mathbf{\Omega}(4k+1,k+1+n)=\mu\bar{\lambda}^4\left[\theta_{22,n}\frac{\sinh(\beta_n\bar{\xi})}{\cosh\,\beta_n}+\theta_{24,n}\frac{\mathrm{sn}(\gamma_n\bar{\xi})}{\mathrm{cs}\,\gamma_n}\right]\cos\,n\pi\bar{\eta}. \tag{A.17}$$

$$\mathbf{\Omega}(4k+1,2k+m)=\mu\bar{\lambda}^4\left[\theta_{11,m}\frac{\cosh(\beta_m\bar{\eta}^*)}{\sinh\,\beta_m}+\theta_{13,m}\frac{\mathrm{cs}(\gamma_m\bar{\eta}^*)}{\mathrm{sn}\,\gamma_m}\right]\sin\,\imath\bar{m}\pi\bar{\xi}. \tag{A.18}$$

$$\mathbf{\Omega}(4k+1,k3+1+n)=\mu^2\bar{\lambda}^4\left[\theta_{41,n}\frac{\cosh\left(\beta_n\bar{\xi}^*\right)}{\cosh\,\beta_n}+\theta_{43,n}\frac{\mathrm{cs}\left(\gamma_n\bar{\xi}^*\right)}{\mathrm{cs}\,\gamma_n}\right]\cos\,n\pi\bar{\eta}. \tag{A.19}$$

$$\mathbf{\Omega}(4k+1,4k+1)=\mu\bar{\lambda}^4\left[\sum_{m=1}^{k}\sum_{n=0}^{k-1}a'_{mn}\sin\,\imath\bar{m}\pi\bar{\xi}\cos\,n\pi\bar{\eta}\right]-1. \tag{A.20}$$

$$\mathbf{\Omega}(m,4k+1)=-\sum_{n=0}^{k-1}a'_{mn}[(n\pi)^2+v(\phi\imath\bar{m}\pi)^2]\cos\,n\pi. \tag{A.21}$$

$$\mathbf{\Omega}(2k+m,4k+1)=-\sum_{n=0}^{k-1}a'_{mn}[(n\pi)^2+v(\phi\imath\bar{m}\pi)^2]. \tag{A.22}$$

$$\mathbf{\Omega}(2k+m,4k+1)=-\sum_{n=0}^{k-1}a'_{mn}[(n\pi)^2+v(\phi\imath\bar{m}\pi)^2]. \tag{A.23}$$

$$\mathbf{\Omega}(k+n+1,4k+1)=-\sum_{m=1}^{k}a'_{mn}[(\imath\bar{m}\pi)^2+v(n\pi/\phi)^2]\sin\,\imath\bar{m}\pi. \tag{A.24}$$

$$\mathbf{\Omega}(3k+n+1,4k+1)=\sum_{m=1}^{k}a'_{mn}\imath\bar{m}\pi. \tag{A.25}$$

To compute the non-zero elements of matrix $\mathbf{\Omega}$ in Eq. (25) using the above equations, one need to evaluate eight types of integrals: $I_{1,mn}$, $I_{2,mn}$,…, and $I_{8,mn}$. They are defined as follows:

$$I_{1,mn}=\frac{2}{\cosh\,\beta_n}\int_0^1\sinh(\beta_n\xi)\sin(\imath\bar{m}\pi\xi)\,\mathrm{d}\xi. \tag{A.26}$$

$$I_{2,mn}=\frac{2}{\mathrm{cs}\,\gamma_n}\int_0^1\mathrm{sn}(\gamma_n\xi)\sin(\imath\bar{m}\pi\xi)\,\mathrm{d}\xi. \tag{A.27}$$

$$I_{3,mn} = \frac{2}{\cosh\ \beta_n} \int_0^1 \cosh(\beta_n \xi^*) \sin(\bar{m}\pi\xi)\, \mathrm{d}\xi. \tag{A.28}$$

$$I_{4,mn} = \frac{2}{\mathrm{cs}\,\gamma_n} \int_0^1 \mathrm{cs}\left(\gamma_n \xi^*\right) \sin(\bar{n}\pi\xi)\, \mathrm{d}\xi. \tag{A.29}$$

$$I_{5,nm} = \frac{2}{\sinh\ \beta_m} \int_0^1 \cosh(\beta_m \eta)\ \cos(n\pi\eta)\, \mathrm{d}\eta \quad \text{for } n \geqslant 1, \quad \frac{1}{\beta_0} \quad \text{for } n = 0. \tag{A.30}$$

$$I_{6,nm} = \frac{2}{\mathrm{sn}\,\gamma_m} \int_0^1 \mathrm{cs}(\gamma_m \eta) \cos(n\pi\eta)\, \mathrm{d}\eta \quad \text{for } n \geqslant 1, \quad \frac{1}{\gamma_0} \quad \text{for } n = 0. \tag{A.31}$$

$$I_{7,nm} = \frac{2}{\sinh\ \beta_m} \int_0^1 \cosh(\beta_m \eta^*) \cos(n\pi\eta)\, \mathrm{d}\eta \quad \text{for } n \geqslant 1, \quad \frac{1}{\beta_0} \quad \text{for } n = 0. \tag{A.32}$$

$$I_{8,nm} = \frac{2}{\mathrm{sn}\,\gamma_m} \int_0^1 \mathrm{cs}(\gamma_m \eta^*) \cos(n\pi\eta)\, \mathrm{d}\eta \quad \text{for } n \geqslant 1, \quad \frac{1}{\gamma_0} \quad \text{for } n = 0. \tag{A.33}$$

References

[1] H.A. Sodano, D.J. Inman, G. Park, A review of power harvesting from vibration using piezoelectric materials, *The Shock and Vibration Digest* 36 (3) (2004) 197–205.

[2] S.R. Anton, H.A. Sodano, A review of power harvesting using piezoelectric materials (2003–2006), *Smart Materials and Structures* 16 (2007) 1–21.

[3] P.M. Ciancio, C.A. Rossit, P.A.A. Laura, Approximate study of the free vibrations of a cantilever anisotropic plate carrying a concentrated mass, *Journal of Sound and Vibration* 302 (2007) 621–628.

[4] A.W. Leissa, The historical bases of the Rayleigh and Ritz methods, *Journal of Sound and Vibration* 287 (2005) 961–978.

[5] R.K. Singhal, D.J. Gorman, Effects of attached masses on free vibration of rigid point supported rectangular plates, *AIAA Journal* 30 (1992) 853–855.

[6] M. Chiba, T. Sugimotob, Vibration characteristics of a cantilever plate with attached spring-mass system, *Journal of Sound and Vibration* 260 (2003) 237–263.

[7] D.J. Gorman, Free vibration analysis of cantilever plates by the method of superposition, *Journal of Sound and Vibration* 49 (4) (1976) 453–467.

[8] S.D. Yu, W.L. Cleghorn, R.G. Fenton, Free vibration and buckling of symmetric cross-ply rectangular laminates, *AIAA Journal* 32 (11) (1994) 2300–2308.

[9] D.J. Gorman, *The Free Vibration Analysis of Rectangular Plates*, Elsevier North Holland, Inc., New York, 1982.

[10] H. Reismann, *Elastic Plates*, Wiley, New York, 1988.